MINOS Observations of Shadowing in the Muon Flux Underground

E.W. Grashorn*† for the MINOS Collaboration
*School of Physics and Astronomy, University of Minnesota, Minneapolis, MN 55455
†Center for Cosmology and AstroParticle Physics, Ohio State University, Columbus, OH 43210

Abstract. **The shadowing of cosmic ray primaries by the disks of the moon and sun has been seen by the MINOS Far Detector at a depth of 2070 mwe using 83.54 million cosmic ray muons accumulated over 1849.48 live-days. The shadow of the moon was observed at the 5.5 σ level and the shadow of the sun at the 4.5 σ using a log-likelihood search in celestial coordinates. This two dimensional shadowing distribution was used to quantify the absolute pointing of the detector on the sky to be $0.174 \pm 0.105^{\circ}$.**

I. Introduction & Motivation

The MINOS Far Detector [1] is a magnetized scintillator and steel tracking calorimeter, located in the Soudan Mine in northern Minnesota, USA, at a depth of 2070 mwe. While primary function of the Far Detector is to detect neutrinos from Fermilab's ν_μ beam, the great depth and wide acceptance of the detector combined with the flat overburden of the Soudan site allow it to serve as a cosmic-ray muon detector as well. The detector is composed of 486 8 m octagonal planes 2.54 cm thick, spaced 5.96 cm. This 5.4 kton detector is 30 m long and has a total aperture of 6.91×10^6 cm^2 sr for this analysis [2]. The Far Detector has a magnetic field that focuses muons from charged-current ν_μ beam interactions and measures momentum from curvature.

Optical telescopes use a standard catalog of stars to establish the resolution and pointing reliability of a new instrument. This is not possible for a cosmic ray detector, as there are no cosmic ray sources available for calibration. There is a well observed phenomena in the otherwise isotropic cosmic ray sky, though it is a deficit, not a source. It is important for cosmic ray and neutrino point source searches to study the resolution and pointing of a cosmic ray detector, and the moon provides a means for this because it absorbs incident cosmic rays, causing deficits from its location. The physical extent and shape of the deficit gives information about the resolution of the detector, while the location of the deficit center gives information about the absolute pointing of the detector. The moon has a 0.5° diameter as viewed from Earth, and the cosmic ray deficit it causes has been measured by air shower arrays (CYGNUS [3], CASA [4], Tibet [5], Milagro [6]), as well as underground detectors (Soudan 2 [7], MACRO [8], [9], L3+C [10]).

MINOS observes underground muons with a minimum energy of 0.7 TeV, and the sharply peaked energy spectrum has a mean value of about 1.0 TeV. This mean energy corresponds to a mean primary energy of about 10 TeV. The moon deficit is affected by phenomena associated with cosmic ray propagation and interaction resulting from geomagnetic fields, Interplanetary Magnetic Fields (IMF), multiple Coulomb scattering, etc [7]. Multiple Coulomb scattering occurs in the rock and causes a general spreading of the moon deficit disc. The geomagnetic field is nearly a dipole, and causes an eastward deflection of positive primaries, which results in a relative east-west shift in the observed shadow of magnitude $\Delta\theta$=1.7$^{\circ} Z/E_p(TeV)$ [11], [12]. The IMF is caused by the sun, which has an ambient dipole field that is 100 times greater than the geomagnetic field. This field is carried through the solar system by the solar wind, the stream of energetic charged particles that emanate from the atmosphere of the sun. Since the sun has a 27 day rotation period, the magnetic field that is carried by the solar wind has a spiral shape, called a Parker spiral [13]. The IMF causes deflection of primaries that strongly depends on the solar wind, and its complex shape makes it very hard to model. The IMF causes a deflection that smears the moon's

shadow, though this effect is small since a primary travels a relatively short distance from the moon to Earth.

II. DATA

A. Event Selection

This analysis encompassed events recorded over 1980 days, from August 1, 2003 - December 31, 2008, for a total of 1849.5 live-days. The data set includes 83.54 million cosmic ray induced muon tracks. required to ensure that the detector was in a reliable state when the data was taken (Pre-Analysis cuts) and that only well reconstructed tracks were included in the sample (Analysis cuts). The Pre-Analysis cuts are described in [14].

Analysis Cuts:

1) "Track Length $<$ 1.55 m", any event with a track shorter than 1.55 m may not be reliably reconstructed.
2) "Number of Planes $<$ 10", a track that passes fewer planes may not give reliable strip information to the track fitter.
3) "$\Delta(\sigma_{vtx}, \sigma_{end})$ >0.021" If the endpoint position is well known but the vertex is not, then the muon has questionable reconstruction pointing.

These cuts were optimized for pointing [15].

A total of 62.6% of the initial 83.54 million triggers survived all cuts, for a total of 52.3 million muons.

III. MOON SHADOW

The one dimensional space angle separation [16] from the location of the moon [17] was found for each muon. The reconstructed muon angular separation from the moon, $\Delta\theta$, was binned in $S_{\rm bin}$ =0.10° increments. Since radial distance from the center of the moon is measured over a two dimensional projection, the solid angle of bin (i) increases when moving out from the center as $\Delta\Omega_i = (2i-1)\cdot S_{\rm bin}^2\pi$. Weighting the number of events in each bin by the reciprocal of the area resulted in the distribution $N_i/\Delta\Omega_i$, the differential muon density. The distribution is a function of the form [18]:

$$\frac{\Delta N_\mu}{\Delta\Omega} = \lambda\left[1 - \frac{R_m^2}{2\sigma^2}e^{-\theta^2/2\sigma^2}\left(1 + \frac{(r^2-2\sigma^2)R_M^2}{8\sigma^4} + \frac{(r^4-8r^2\sigma^2+8\sigma^4)R_M^4}{192\sigma^8}\right)\right] \quad (1)$$

where λ is the average differential muon flux, σ accounts for smearing from detector resolution, multiple Coulomb scattering and geomagnetic deflection, and R_m =0.26°, the radius of the moon. A fit to Eq. 1 yields χ^2_G/ndf =36.6/38 with

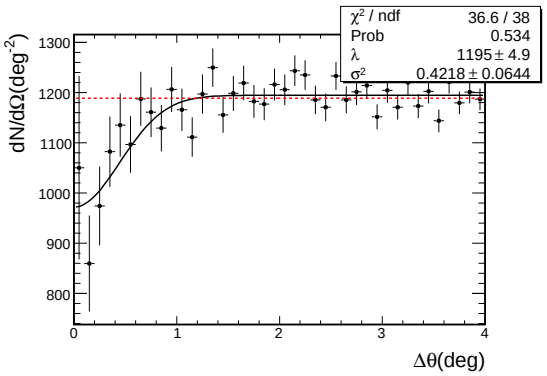

Fig. 1. The differential muon flux with respect to displacement from the moon's location, binned in 0.1°. The dashed curve is the result of a linear (no moon) fit ($\chi^2_L/ndf = 55.1/39$), while the solid curve is the best fit from Eq. 1 ($\chi^2_G/ndf = 36.4/38$). The Gaussian (moon-induced deficit) fit gives parameters $\lambda = 1195 \pm 4.9$ and $\sigma = 0.42 \pm 0.06°$.

parameters λ =1195±4.9 and σ =0.42±0.06°, an improvement of 23.7 over the linear fit (χ^2_L/ndf =59.3/39). This change in χ^2 corresponds to a 6×10^{-6} chance probability.

A two dimensional maximum likelihood grid search assumes no particular location of the moon and so is a more powerful tool to assess absolute detector pointing. The Far Detector Point Spread Function (PSF) is specific to the type, geometry and amount of rock overburden, which determines the energy at which muons are sampled, the geometry of the detector, and other smearing effects. Dimuon events offer a means to determine the point spread function since they are created with nearly parallel trajectories. The resulting distribution of separation angles at the detector automatically accounts for these smearing effects [15]. The distribution of single muon separation angles from dimuon events was used

to find the Far Detector point spread function in celestial coordinates (Right Ascension (RA), and Declination (Dec)). Scaling ΔRA by $\cos$(Dec) accounts for the differing solid angle subtended by an RA separation at a given Dec. This is the distribution of expected smearing of muon tracks in the Far Detector. A simple *Monte Carlo* was written to quantify the expected scattering about the moon by sending muons toward a 0.5° disk. If the muon fell in the region of the disk, it was excluded; if not, an angular separation was selected at random from the PSF. The resulting deficit the expected effect of the moon on Cosmic Ray primaries observable in the Far Detector.

One thousand background samples of the isotropic cosmic ray sky were generated using the method in [15]. These were averaged to create a smooth, isotropic background grid, sorted in equal solid angle bins 0.10° on a side. The data were sorted in a similar grid. A grid search utilizing a log-likelihood method was employed to find the most probable position of a moon-like deficit. This method was invented by Cash [19], first applied by COS-B [20], and first applied to the moon shadow by MACRO [8]. The moon template was placed at a fixed position (x,y) on the grid, and the shadowing source with strength I_s at fixed position (x_s,y_s) that fits the data best was found by minimizing:

$$\chi^2(x,y,I_s) = 2\sum_{i=1}^{n_{bin}} \left[N_i^{th} - N_i^{obs} + N_i^{obs} \ln \frac{N_i^{obs}}{N_i^{th}} \right], \quad (2)$$

where $N_i^{th} = N_i^{back} I_s(x,y)$, N_i^{back} is the number of muons from the smoothed background grid for (x,y). To determine the strength of this deficit, the parameter Λ was defined as:

$$\Lambda = \chi^2(x,y,0) - \chi^2(x,y,I_s), \quad (3)$$

which is a measure of the deviation from the null (no-moon) hypothesis. The data grid is fit with a template of shadowing depth I_s, which includes *a priori* assumptions of the existence and radius of the moon.

The two dimensional distribution of these deviations was drawn on a $2^\circ \times 2^\circ$ grid, binned in 0.01° on a side, and can be seen in Fig. 2(L) in celestial coordinates. The greatest deficit is $\Lambda = 29.8$, centered on $(-0.13 \pm 0.081^\circ, -0.17 \pm 0.11^\circ)$. The distribution of Λ is the same as for a $\chi^2(\nu)$ distribution [19]. In this case there is only one free parameter, I_s, so Λ=29.8 has a χ^2 probability of 6×10^{-8} (5.5σ).

IV. Sun Shadow

The two dimensional log-likelihood analysis described in Sec. III was performed for separation of cosmic muons from the location of the sun. As viewed from Earth, the sun obscures a 0.5° diameter disk, the same size as the moon. Historically, this has been a more difficult [9] measurement to make for reasons already mentioned in Sec. I. The two dimensional sun shadow can be seen in Fig. 2(R). The sun $\Lambda_{max} = 19.3$ centered on $(-0.19 \pm 0.10^\circ, 0.16 \pm 0.11^\circ)$, which has a χ^2 probability of 6×10^{-6} (4.5σ).

V. Conclusions

Using 52.3 million muons accumulated over 1845.9 live-days, the MINOS Far Detector has observed the cosmic ray shadow of the moon with a high significance. The two dimensional moon shadow was found with a significance of 6×10^{-8} (5.5 σ), centered on $(-0.13 \pm 0.081^\circ, -0.17 \pm 0.11^\circ)$, which suggests that the absolute pointing of the detector on the sky is known to $0.17 \pm 0.11^\circ$. The two dimensional sun shadow was found with a significance of 6×10^{-6} (4.5 σ), centered on $(-0.19 \pm 0.10^\circ, 0.16 \pm 0.11^\circ)$.

VI. Acknowledgments

We thank the Fermilab staff and the technical staffs of the participating institutions for their vital contributions. This work was supported by the U.S. Department of Energy, the U.S. National Science Foundation, the U.K. Science and Technologies Facilities Council, the State and University of Minnesota, the Office of Special Accounts for Research Grants of the University of Athens, Greece, FAPESP (Rundacao de Amparo a Pesquisa do Estado de Sao Paulo), CNPq (Conselho Nacional de Desenvolvimento Cientifico e Tecnologico) in Brazil. We gratefully acknowledge the Minnesota Department of Natural Resources for their assistance and for allowing us access to the facilities of the Soudan Underground Mine State Park and the crew of the Soudan Underground Physics laboratory for their tireless work in building and operating the MINOS detector.

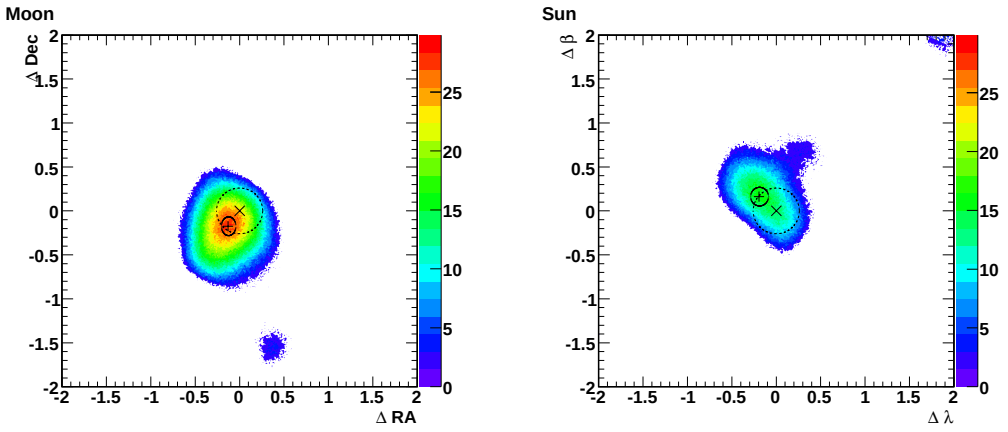

(a) Moon Shadow (b) Sun Shadow

Fig. 2. The two dimensional moon induced muon deficit (L) and sun induced deficit (R) in $0.01\,\mathrm{deg}^2$ bins, in celestial coordinates. The cross marks the best fit location of moon(sun), and the ellipse surrounding the cross mark the uncertainty in that position. The X marks the expected location of the moon (sun), and the circle is the apparent size of the moon (sun) as veiwed from earth. The greatest deficit in the moon plot is $\Lambda = 29.8$, a $5\,\sigma$ chance probability, centered on $(-0.13^\circ, -0.17^\circ)$ The greatest deficit in the sun plot is $\Lambda_{sun} = 19.3$, a $4.5\,\sigma$ chance probability, centered on $(-0.19^\circ, 0.16^\circ)$.

REFERENCES

[1] D. G. Michael, et al., The magnetized steel and scintillator calorimeters of the MINOS experiment, Nucl Instr. & Meth. A 596 (2008) 190–228.

[2] B. J. Rebel, Neutrino induced muons in the MINOS far detector PhD Dissertation, Indiana University FERMILAB-THESIS-2004-33.

[3] D. E. Alexandreas, et al., Observation of shadowing of ultrahigh-energy cosmic rays by the moon and the sun, Phys. Rev. D43 (1991) 1735–1738.

[4] A. Borione, et al., Observation of the shadows of the moon and sun using 100- tev cosmic rays, Phys. Rev. D49 (1994) 1171–1177.

[5] M. Amenomori, et al., Cosmic ray deficit from the directions of the moon and the sun detected with the tibet air shower array, Phys. Rev. D47 (1993) 2675–2681.

[6] R. W. Atkins, et al., Milagrito, a TeV air-shower array, Nucl. Instrum. Meth. A449 (2000) 478–499.

[7] J. H. Cobb, et al., The observation of a shadow of the moon in the underground muon flux in the soudan 2 detector, Phys. Rev. D61 (2000) 092002.

[8] M. Ambrosio, et al., Observation of the shadowing of cosmic rays by the moon using a deep underground detector, Phys. Rev. D59 (1999) 012003.

[9] M. Ambrosio, et al., Moon and sun shadowing effect in the macro detector, Astropart. Phys. 20 (2003) 145–156.

[10] P. Achard, et al., Measurement of the shadowing of high-energy cosmic rays by the moon: A search for tev-energy antiprotons, Astropart. Phys. 23 (2005) 411–434.

[11] M. Urban, P. Fleury, R. Lestienne, F. Plouin, Can we detect antimatter from other galaxies by the use of the earth's magnetic field and the moon as an absorber?, Nucl. Phys. Proc. Suppl. 14B (1990) 223–236.

[12] J. Heintze, et al., Measuring the chemical composition of cosmic rays by utilizing the solar and geomagnetic fieldsIn *Adelaide 1990, Proceedings, Cosmic ray, vol. 4* 456- 459.

[13] E. N. Parker, Dynamics of interplanetary gas and magnetic fields, Astrophys. J. 128 (1958) 664.

[14] P. Adamson, et al., Measurement of the atmospheric muon charge ratio at tev energies with minos, Phys. Rev. D76 (2007) 052003.

[15] E. W. Grashorn, Astroparticle physics with the minos far detectorPhD Dissertation, University of Minnesota FERMILAB-THESIS-2008-06.

[16] R. Sinnott, Virtues of the haversine, Sky and Telescope 68 (2).

[17] E. Standish, JPL planetary and lunar ephemerides, JPL IOM 312.F-98-04B.

[18] P. Adamson, et al., MINOS MINOS Observations of Shadowing in the Muon Flux Underground, to be submitted to Astropart. Physics.

[19] W. Cash, Parameter estimation in astronomy through application of the likelihood ratio, Astrophys. J. 228 (1979) 939–947.

[20] A. M. T. Pollock, et al., COS-B gamma-ray sources and interstellar gas in the first galactic quadrant - caravane collaboration for the COS-B satellite, Astronomy and Astrophysics 146 (1985) 352–362.